

# One-loop electroweak radiative corrections to polarized $e^+e^- \rightarrow \gamma Z$ process

S. Bondarenko<sup>1,2</sup>, Ya. Dydyshka<sup>3,4</sup>, L. Kalinovskaya<sup>3</sup>, L. Rummyantsev<sup>3</sup>,  
R. Sadykov<sup>3</sup>, and V. Yermolchyk<sup>3,4</sup>

<sup>1</sup>Bogoliubov Laboratory of Theoretical Physics, JINR, 141980 Dubna, Moscow region, Russia

<sup>2</sup>Dubna State University, Universitetskaya str. 19, 141980 Dubna, Russia

<sup>3</sup>Dzhelepov Laboratory of Nuclear Problems, JINR, 141980 Dubna, Moscow region, Russia

<sup>4</sup>Institute for Nuclear Problems, Belarusian State University, Minsk, 220006, Belarus

## Abstract

This paper gives high-precision theoretical predictions for cross sections of the process  $e^+e^- \rightarrow \gamma Z$  for future electron-positron colliders. The calculations are performed using the **SANC** system. They include complete one-loop electroweak radiative corrections, as well as longitudinal polarization of the initial state. Numerical results are given for the center-of-mass system energy range  $\sqrt{s} = 250 - 1000$  GeV with various polarization degrees in the  $\alpha(0)$  and  $G_\mu$  EW schemes. This study is a contribution to the research program of the CEPC project being under development in China.

## 1 Introduction

Clean experimental conditions, negligible pile-up and controlled centre-of-mass energy, part-per-mil accuracy for cross sections for signal and background processes, and well-understood backgrounds for final states are assumed at future  $e^+e^-$  colliders. All this allows us to search for new physics by accurately measuring deviations from the Standard Model [1, 2]. However, there are challenges that arise from the very richness of the  $e^+e^-$  program. One needs to match theoretical accuracy with the statistical one taking into account electroweak (EW) radiative corrections (RCs) [3].

Modern evaluation tools to estimate theoretical uncertainties for future  $e^+e^-$  colliders, i.e., FCCee [4, 5], ILC [6–8], CLIC [9], CEPC [10, 11] should be applied. An important advantage of linear collider ILC and CLIC is planned high degree of polarization of electron beams. Polarized beams can improve opportunities for investigation of the fundamental particle properties [2, 4, 7, 12, 13].

In the physical programs for the future  $e^+e^-$  colliders significant attention devoted to the  $e^+e^- \rightarrow \gamma Z$  process. All of them have options to operate at centre-of-mass energies

in the range 240–250 GeV, and are expected to accumulate about  $10^5 - 10^6$  Higgs boson events.

At this energy the dominant Higgs production channel is the Higgsstrahlung process  $e^+e^- \rightarrow HZ$  [14]. Because of clear initial  $e^+e^-$  state it is possible to identify Higgs boson events independently of the decay mode, and the largest background comes from two processes  $e^+e^- \rightarrow \gamma Z$  and  $e^+e^- \rightarrow ZZ$ .

Also it is supposed to precisely calibrate the energy scales of the particles using the  $e^+e^- \rightarrow \gamma Z$  process for measuring Higgs boson coupling constants [15], and for evaluating the left-right asymmetry at the center-of-mass energy of 250 GeV [16, 17].

An accurate measurement of the number of neutrinos is proposed by using the radiative return to the Z boson,  $e^+e^- \rightarrow \gamma Z$  [5].

Here, we focus on the evaluation and analysis of the effects associated with the longitudinal polarization of the initial beams of the process  $e^+e^- \rightarrow \gamma Z$ .

This is the second part of the study of theoretical uncertainties of the process [18]

$$\begin{aligned} e^+(p_1, \chi_1) + e^-(p_2, \chi_2) &\rightarrow \\ &\rightarrow \gamma(p_3, \chi_3) + Z(p_4, \chi_4) (+\gamma(p_5, \chi_5)) \end{aligned} \quad (1)$$

at the complete one-loop electroweak level in **SANC**, with  $p_i, \chi_i$  being the momentum and helicity of the  $i$ th particle.

In our previous paper [18] the relevant contributions for one-loop corrections, i.e., Born, virtual and real photon bremsstrahlung, to the cross section were calculated analytically, the independence of the form factors of gauge parameters was tested, and the stability of the result on the variation of the soft-hard separation parameter  $\bar{\omega}$  was checked. We keep all masses and operate in full phase space. All calculations were carried out via the **MCSANcEe** [19] integrator and the **ReneSANCe** generator [20].

One-loop QED and EW RCs to the unpolarized  $e^+e^- \rightarrow \gamma Z$  process were previously calculated in [21–24]. However, it is difficult to draw a direct comparison between our results and these papers due to incomplete setups.

The article is organized as follows. Section 2 describes the general notations. Numerical results and comparison are presented in Section 3. A summary is given in Section 4.

## 2 Differential cross section

To study the case of the longitudinal polarization with degrees  $P_{e^+}$  and  $P_{e^-}$ , we produce helicity amplitudes and make a formal application of Eq. (1.15) from [12]:

$$\sigma(P_{e^+}, P_{e^-}) = \frac{1}{4} \sum_{\chi_1, \chi_2} (1 + \chi_1 P_{e^+})(1 + \chi_2 P_{e^-}) \sigma_{\chi_1 \chi_2}, \quad (2)$$

where  $\chi_i = -1(+1)$  corresponds to the particle  $i$  with the left (right) helicity.

The cross section of the process at the one-loop level can be divided into four parts:

$$\sigma^{\text{one-loop}} = \sigma^{\text{Born}} + \sigma^{\text{virt}}(\lambda) + \sigma^{\text{soft}}(\lambda, \bar{\omega}) + \sigma^{\text{hard}}(\bar{\omega}),$$

where  $\sigma^{\text{Born}}$  is the Born cross section,  $\sigma^{\text{virt}}$  is the contribution of virtual (loop) corrections,  $\sigma^{\text{soft}}$  is the contribution of soft photon emission,  $\sigma^{\text{hard}}$  is the contribution of hard photon emission (with energy  $E_\gamma > \bar{\omega}$ ). Auxiliary parameters  $\lambda$  ("photon mass") and  $\bar{\omega}$  (soft-hard separator) are canceled after summation.

### 3 Numerical results and comparisons

To estimate the theoretical uncertainties we consider results calculated in the  $\alpha(0)$  and  $G_\mu$  EW schemes. Numerical results for NLO (next-to-leading-order) EW RCs involve the one-loop cross sections, corresponding angular and energy distributions, the polarization effect for the following longitudinally polarized states of the positron ( $P_{e^+}$ ) and electron ( $P_{e^-}$ ) beams

$$(P_{e^+}, P_{e^-}) = (0, 0), (-1, +1), (+1, -1), \\ (0.3, -0.8), (-0.3, 0.8), (0, -0.8), (0, 0.8)$$

and set of center-of-mass (c.m.) energies

$$\sqrt{s} = 250, 500, 1000 \text{ GeV}. \quad (3)$$

The following setup of input parameters is used:

$$\begin{aligned} \alpha(0) &= 1/137.03599976, & G_\mu &= 1.16637 \times 10^{-5} \text{ GeV}^{-2}, \\ M_Z &= 91.1876 \text{ GeV}, & \Gamma_Z &= 2.49977 \text{ GeV}, \\ M_W &= 80.451495 \text{ GeV} & M_H &= 125.0 \text{ GeV}, \\ m_e &= 0.5109990 \text{ MeV}, & m_\mu &= 0.105658 \text{ GeV}, \\ m_\tau &= 1.77705 \text{ GeV}, \\ m_u &= 0.062 \text{ GeV}, & m_d &= 0.083 \text{ GeV}, \\ m_c &= 1.5 \text{ GeV}, & m_s &= 0.215 \text{ GeV}, \\ m_t &= 173.8 \text{ GeV}, & m_b &= 4.7 \text{ GeV}. \end{aligned}$$

In the calculations, the following cuts were imposed:

- c.m. angular cuts for the Born, soft and virtual contributions where there is only one photon in the final state  $\cos \vartheta_\gamma \in [-0.9, 0.9]$
- for the hard contribution of both photons must have a c.m. energy greater than  $\bar{\omega}$ ;
- for the hard event to be accepted,  $\cos \vartheta_Z$  and at least one photon  $\cos \vartheta_{\gamma_1}, \cos \vartheta_{\gamma_2}$  must lie within the interval  $[-0.9, 0.9]$ .

It should be noted that this coincides with the criteria which were used in [18].

#### 3.1 Triple comparison of the tree level results: Born and hard photon bremsstrahlung cross sections

Here we compare for fully polarized Born and hard photon bremsstrahlung cross sections with the ones obtained via the `CalcHEP` [25] and `WHIZARD` [26, 27] codes. The results are given within the  $\alpha(0)$  EW scheme with any photon energy  $E_\gamma > \bar{\omega}$ ,  $\bar{\omega} = 10^{-4} \sqrt{s}/2$  and fixed 100% polarized initial beams in the full phase space.

The agreement for the Born cross section was found to be excellent (we omit the corresponding table). Table 1 shows very good agreement between `SANC` results (first row) for the hard photon bremsstrahlung cross section contributions, `CalcHEP` results (second row) and `WHIZARD` results (third row).

Table 1: Tuned triple comparison between SANC (first line), CalcHEP (second line) and WHIZARD (third line) results for the hard bremsstrahlung contributions to polarized  $e^+e^- \rightarrow \gamma Z(\gamma)$  scattering for various degrees of polarization and energies.

$P_{e^+}, P_{e^-}$	-1, -1	-1, +1	+1, -1	+1, +1
$\sigma_{e^+e^-}^{\text{hard}}$ , pb, $\sqrt{s} = 250$ GeV				
S	2.51(1)	69.74(1)	110.09(1)	2.53(1)
C	2.53(1)	69.75(1)	110.09(1)	2.53(1)
W	2.53(1)	69.75(1)	110.07(2)	2.53(1)
$\sigma_{e^+e^-}^{\text{hard}}$ , pb, $\sqrt{s} = 500$ GeV				
S	0.74(1)	17.04(1)	26.89(1)	0.75(1)
C	0.76(1)	17.03(1)	26.88(1)	0.76(1)
W	0.76(1)	17.05(1)	26.90(1)	0.76(1)
$\sigma_{e^+e^-}^{\text{hard}}$ , pb, $\sqrt{s} = 1000$ GeV				
S	0.202(1)	4.604(1)	7.266(1)	0.206(1)
C	0.206(1)	4.603(1)	7.267(1)	0.206(1)
W	0.206(1)	4.603(1)	7.265(1)	0.206(1)

## 3.2 Polarized total cross sections

### 3.2.1 Energy dependence

The corresponding unpolarized/polarized results for the Born and complete one-loop EW cross sections as well as for relative corrections are presented in Table 2. Relative corrections  $\delta^i$  are computed as the ratios of the corresponding one-loop contributions to the Born level cross section for three energies. We only show the components  $\sigma_{-+}$  and  $\sigma_{+-}$  because even in cases of a partly polarized initial state, the polarized cross sections are mainly determined by these components.

Table 2 presents the result of calculating the Born and one-loop cross sections as well as the relative correction  $\delta = \sigma^{\text{one-loop}}/\sigma^{\text{Born}} - 1$  in percent of the  $e^+e^- \rightarrow \gamma Z(\gamma)$  scattering for c.m. energies  $\sqrt{s} = 250, 500$  and  $1000$  GeV in the  $\alpha(0)$  scheme.

It is seen that the QED RCs are about +7.5% and almost constant for the c.m. energies (3), while the weak relative corrections strongly depend on the energy and the degree of the initial beam polarization: they are mostly positive for positive electron polarization and mostly negative for negative electron polarization. The complete EW NLO corrections also strongly depend on the energy and the degree of polarization.

### 3.2.2 Scheme dependence

To assess the theoretical uncertainty, we perform calculations in the  $\alpha(0)$  and  $G_\mu$  EW schemes. The integrated cross sections for the weak corrections in these schemes and their relative difference

$$\delta_{G_\mu/\alpha(0)} = \frac{\sigma_{G_\mu}}{\sigma_{\alpha(0)}} - 1, \% \quad (4)$$

are presented in Table 3.

Table 2: Born and complete one-loop cross sections  $\sigma$  in pb, and relative corrections  $\delta$  in % for the c.m. energies  $\sqrt{s} = 250, 500, 1000$  GeV, at various degree of polarization of the initial particles in the  $\alpha(0)$  EW scheme.

$P_{e^+}, P_{e^-}$	0, 0	-1, +1	+1, -1	0.3, -0.8	-0.3, 0.8	0, -0.8	0, 0.8
$\sqrt{s} = 250$ GeV							
$\sigma^{\text{Born}}$ , pb	4.094(1)	6.353(1)	10.025(1)	6.087(1)	4.067(1)	4.829(1)	3.360(1)
$\sigma^{\text{NLO}}$ , pb	4.489(1)	7.572(1)	10.364(1)	6.332(1)	4.796(1)	5.048(1)	3.931(1)
$\delta^{\text{NLO}}$ , %	9.63(1)	19.19(1)	3.38(1)	4.03(1)	17.92(1)	4.53(1)	16.98(1)
$\delta^{\text{QED}}$ , %	7.63(1)	7.52(1)	7.50(1)	7.57(1)	7.60(1)	7.61(1)	7.65(1)
$\delta^{\text{weak}}$ , %	2.01(1)	11.68(1)	-4.12(1)	-3.55(1)	10.31(1)	-3.08(1)	9.32(1)
$\sqrt{s} = 500$ GeV							
$\sigma^{\text{Born}}$ , pb	0.8335(1)	1.2932(1)	2.0407(1)	1.2391(1)	0.82795(1)	0.98299(1)	0.68398(1)
$\sigma^{\text{NLO}}$ , pb	0.8801(1)	1.5362(1)	1.9811(1)	1.2137(1)	0.9692(1)	0.9696(1)	0.7917(1)
$\delta^{\text{NLO}}$ , %	5.65(1)	18.79(1)	-2.92(1)	-2.05(1)	17.06(1)	-1.37(1)	15.75(1)
$\delta^{\text{QED}}$ , %	7.35(1)	7.21(1)	7.20(1)	7.26(1)	7.33(1)	7.33(1)	7.40(1)
$\delta^{\text{weak}}$ , %	-1.69(1)	11.60(1)	-10.12(1)	-9.33(1)	9.72(1)	-8.69(1)	8.36(1)
$\sqrt{s} = 1000$ GeV							
$\sigma^{\text{Born}}$ , pb	0.19860(1)	0.30813(1)	0.48625(1)	0.29524(1)	0.19728(1)	0.23422(1)	0.16297(1)
$\sigma^{\text{NLO}}$ , pb	0.19747(3)	0.3663(1)	0.4222(1)	0.260154(4)	0.22927(2)	0.20861(2)	0.18625(2)
$\delta^{\text{NLO}}$ , %	-0.57(2)	18.85(1)	-13.17(1)	-11.88(1)	16.22(1)	-10.93(1)	14.28(1)
$\delta^{\text{QED}}$ , %	7.56(1)	7.38(1)	7.39(1)	7.51(1)	7.52(1)	7.55(1)	7.58(1)
$\delta^{\text{weak}}$ , %	-8.13(1)	11.47(1)	-20.55(1)	-19.38(1)	8.71(1)	-18.45(1)	6.70(1)

As is well known, the difference between two EW schemes in the LO is just the ratio of the EW couplings and gives  $\delta_{G_\mu/\alpha(0)}^{\text{LO}} = 6.5\%$ . As seen in the table, the weak contribution reduces the difference to about 0.55% at the energy of 250 GeV, 0.32% at 500 GeV and 0.11% at 1000 GeV. These ratios (4) show stabilization of the results and can be considered as an estimation of the theoretical uncertainty of weak contributions, that is, additional corrections of two and more loops.

### 3.3 Differential distributions

#### 3.3.1 Angular dependence

The angular dependence of the unpolarized cross sections for the Born and one-loop levels in the  $\alpha(0)$  EW scheme (upper panel) and QED and weak relative corrections (lower panel) is illustrated in Figs. 1-3. The symbol  $\vartheta_Z$  denotes the angle between the initial positron  $e^+(p_1)$  and the  $Z$ -boson. This angular curve is symmetrical about zero. For all c.m. energies the minimum of the Born and one-loop cross sections is at zero while the maximum is in the corners of the angular cut value.

At  $\sqrt{s} = 250$  GeV the QED relative corrections dominate and are only modified slightly by weak corrections. But as the energy increases, the situation changes. We observe that at  $\sqrt{s} = 500$  and 1000 GeV both corrections are large, and the strong

Table 3: Integrated Born and weak contributions to the cross section corrections in two EW schemes,  $\alpha(0)$  and  $G_\mu$ , at the center-of-mass energies (3)

$\sqrt{s}$ , GeV	250	500	1000
$\sigma_{\alpha(0)}^{\text{Born}}$ , pb	4.09449(1)	0.83348(1)	0.19860(1)
$\sigma_{G_\mu}^{\text{Born}}$ , pb	4.36105(1)	0.88774(1)	0.21152(1)
$\delta_{G_\mu/\alpha(0)}^{\text{Born}}$ , %	6.51(1)	6.51(1)	6.50(1)
$\sigma_{\alpha(0)}^{\text{weak}}$ , pb	4.17661(1)	0.81936(1)	0.18245(1)
$\sigma_{G_\mu}^{\text{weak}}$ , pb	4.19941(1)	0.82199(1)	0.18225(1)
$\delta_{G_\mu/\alpha(0)}^{\text{weak}}$ , %	0.55(1)	0.32(1)	0.11(1)

compensation occurs.

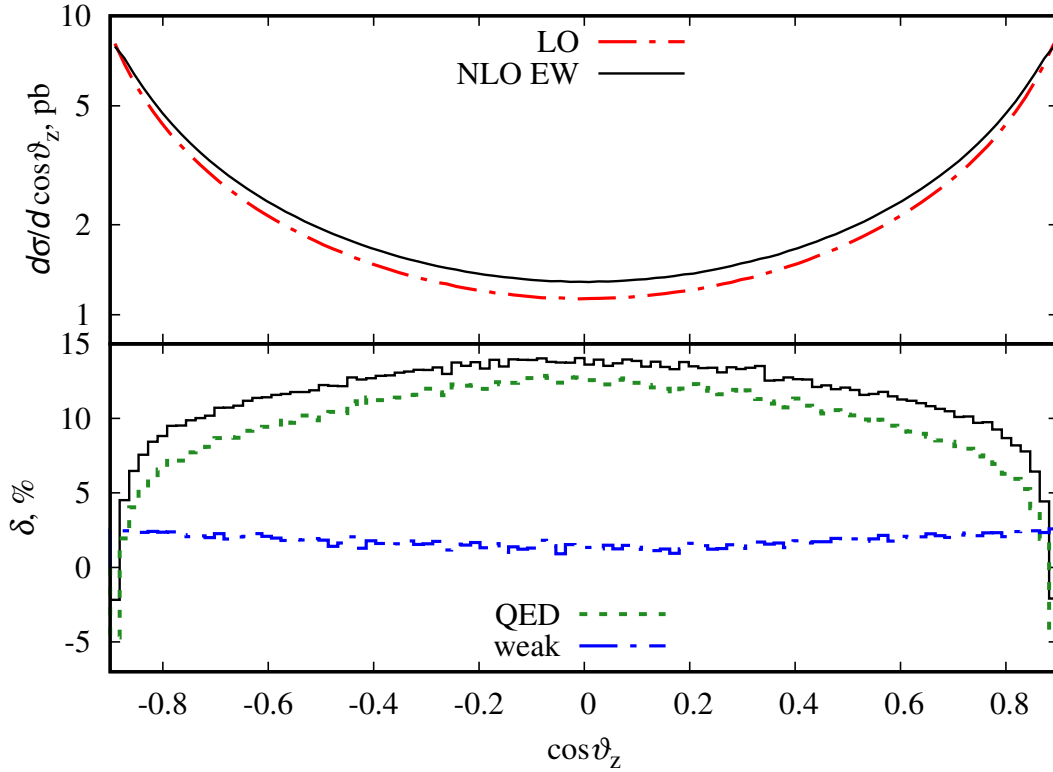


Figure 1: LO and EW NLO (in parts) cross sections and relative corrections at  $\sqrt{s} = 250$  GeV for unpolarized initial beams

In Figs. 4-6, the LO (dashed line) and NLO EW (solid line) cross sections (upper panel) as well as the relative corrections (lower panel) are shown. The red lines correspond (solid/dashed lines) to partially polarized initial beams with  $(P_{e^+}, P_{e^-}) = (\pm 0.3, \mp 0.8)$ . Radiative corrections significantly reduce cross sections at the energy  $\sqrt{s} = 250$  GeV in the whole range of scattering angles. The real planned polarized states in the

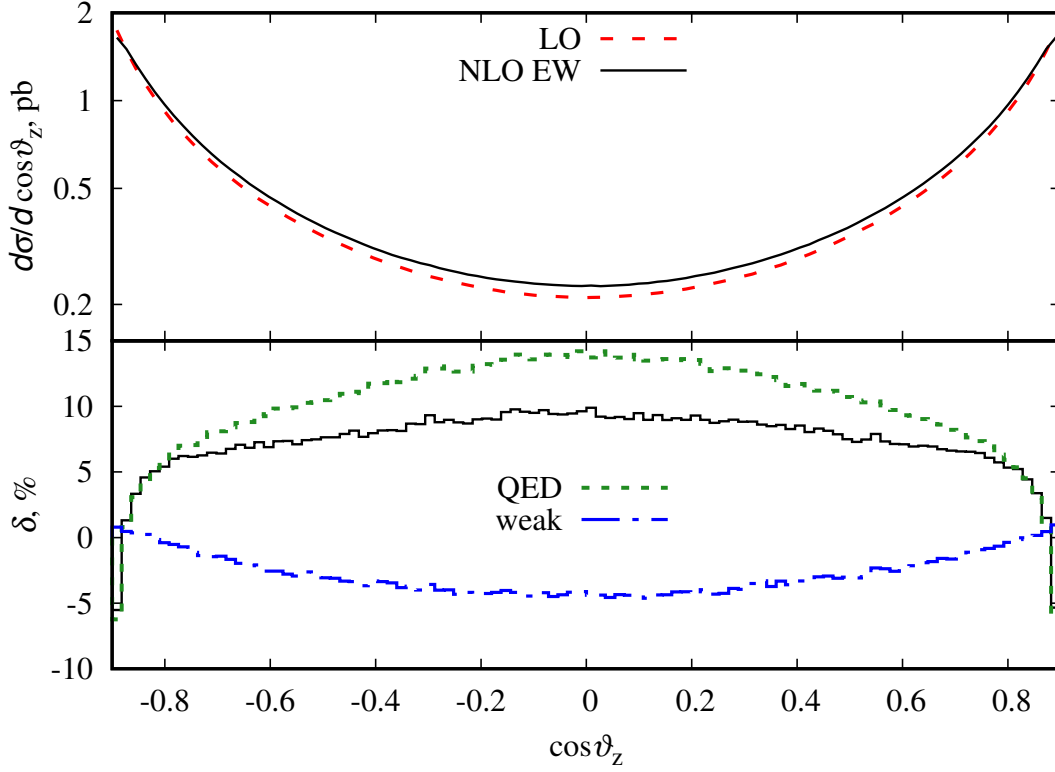


Figure 2: The same as in Fig. 1 but for  $\sqrt{s} = 500$  GeV

ILC experiment show a significant dependence on the polarization of the initial beams, namely, for  $(P_{e^+}, P_{e^-}) = (+0.3, -0.8)$  the relative corrections are from  $-10$  up to  $+5\%$  while for  $(-0.3, +0.8)$  they are from  $5$  to  $23\%$ .

At the c.m. energy  $\sqrt{s} = 500$  GeV the dependence on polarization is also strong, and  $\delta$  is from  $-10\%$  to  $0\%$ . At the c.m. energy  $\sqrt{s} = 1000$  GeV  $\delta$  varies from  $-20\%$  to  $-10\%$  for  $(+0.3, -0.8)$ .

For  $(P_{e^+}, P_{e^-}) = (-0.3, +0.8)$  the radiative corrections vary from  $5\%$  to  $23\%$  and slightly depend on the energy.

It should also be noted that the nonphysical dips in the first and last bins of the relative correction histograms are due to the angular limits and can be removed by applying wider cuts.

### 3.3.2 Energy dependence

The LO and NLO EW corrected unpolarized cross sections in pb as a function of the c.m. energy are shown in Fig. 7. At the bottom of the figure the specific contributions of the relative NLO EW corrections are drawn. We decompose the complete one-loop contribution into two gauge-invariant subsets of the QED and weak diagrams.

In the c.m. energy range from  $100$  to  $200$  GeV, the QED corrections have a sharp

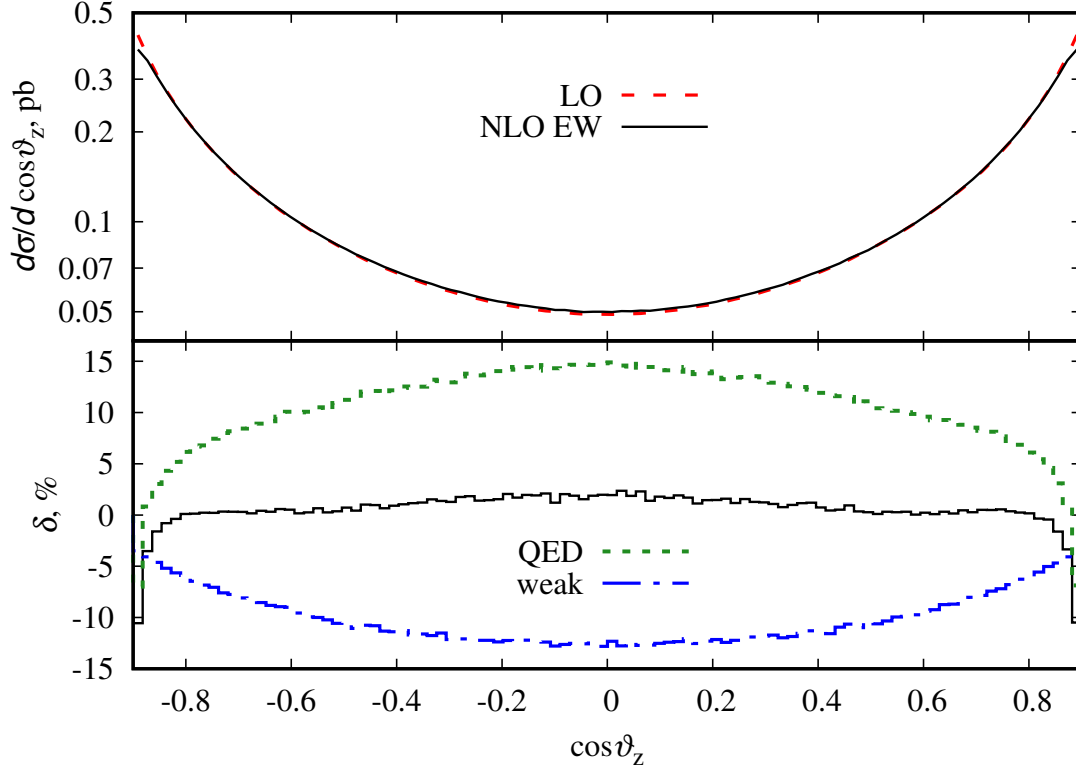


Figure 3: The same as in Fig. 1 but for  $\sqrt{s} = 1000$  GeV

rising from negative (about  $-10\%$ ) to positive (about  $6\%$ ) values and then are practically constant while the weak corrections have a pick corresponding to the under threshold two  $W$ -boson box and then start to decrease.

### 3.4 Left-right asymmetry

The left-right asymmetry shows an order of parity violation and, by definition (5), does not depend on the degrees of the initial beam polarization:

$$A_{LR} = \frac{\sigma_{LR} - \sigma_{RL}}{\sigma_{LR} + \sigma_{RL}}, \quad (5)$$

with  $\sigma_{LR}$  and  $\sigma_{RL}$  being the cross sections for the fully polarized electron-positron  $e_L^- e_R^+$  and  $e_R^- e_L^+$  initial states, respectively. Figure 8 shows the distributions of  $A_{LR}$  in  $\cos\vartheta_Z$  for the Born and one-loop contribution at the c.m. energies  $\sqrt{s} = 250, 500, 1000$  GeV in the  $\alpha(0)$  EW scheme. The corresponding shift of the asymmetry

$$\Delta A_{LR} = A_{LR}(\text{NLO EW}) - A_{LR}(\text{LO})$$

is shown in the lower panel.

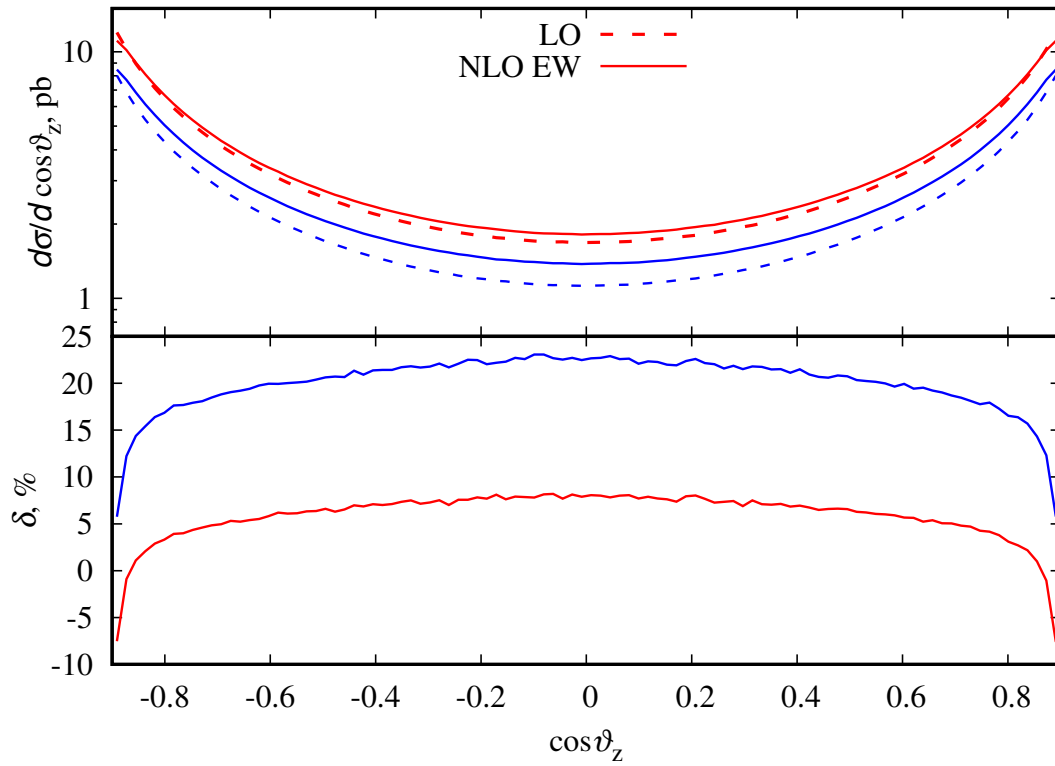


Figure 4: LO and EW NLO cross sections and relative corrections at  $\sqrt{s} = 250$  GeV with polarized initial beams.

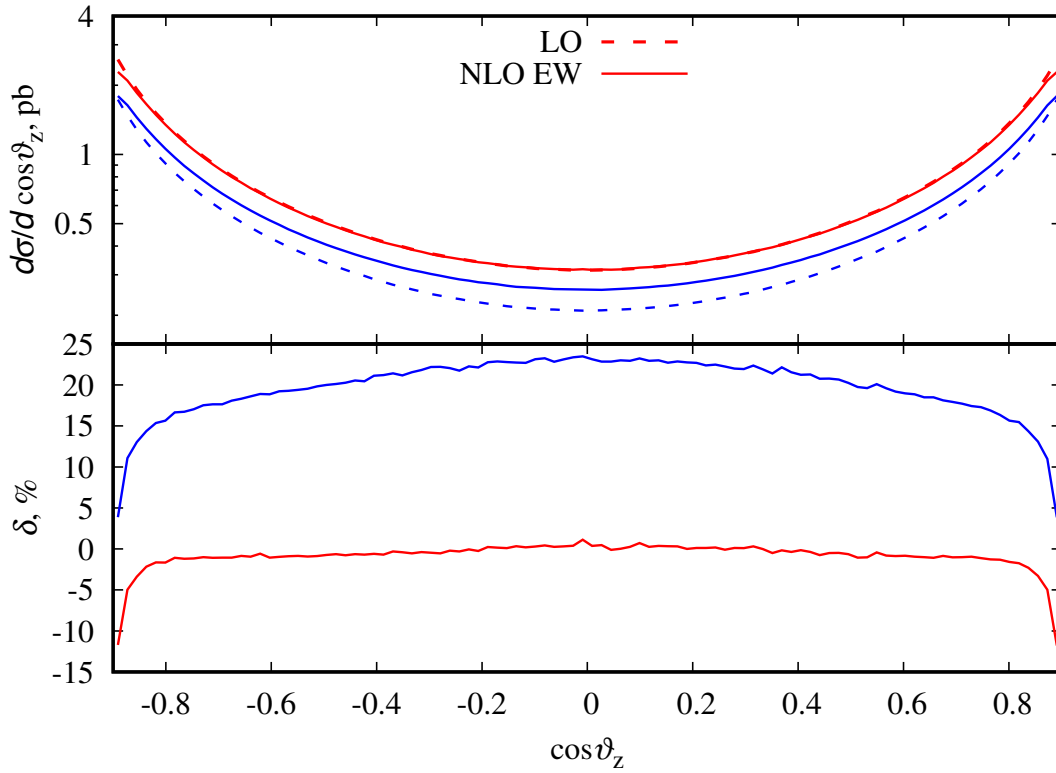


Figure 5: The same as in Fig. 4 but for  $\sqrt{s} = 500$  GeV

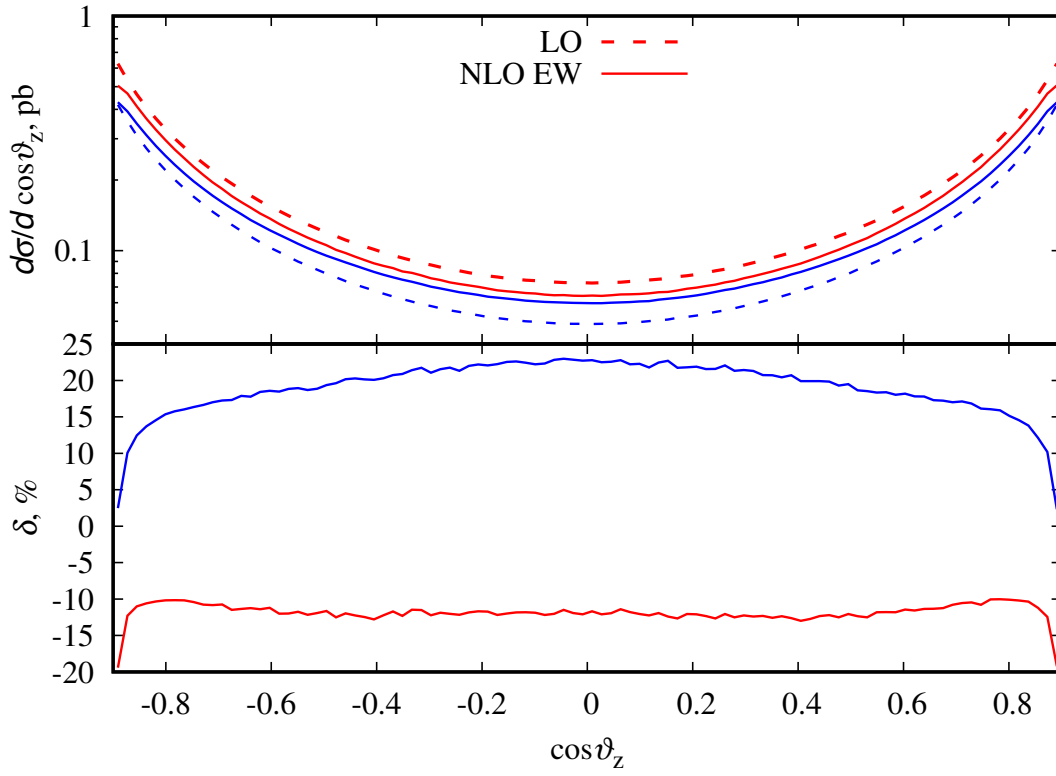


Figure 6: The same as in Fig. 4 but for  $\sqrt{s} = 1000$  GeV

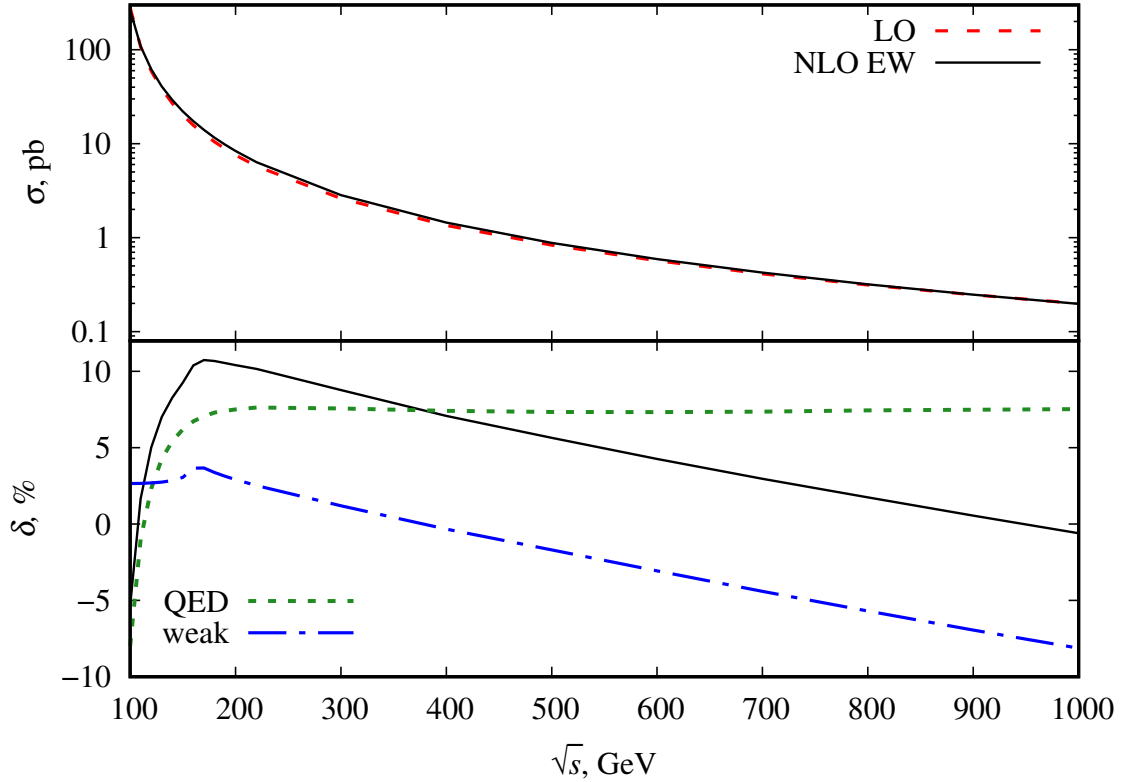


Figure 7: The LO and NLO EW corrected unpolarized cross sections and the relative corrections in parts as a function of the center-of-mass energy.

At Born level,  $A_{LR}$  is constant:

$$A_{LR}^{\text{Born}} = \frac{(1 - 2 \sin^2 \theta_W)^2 - 4 \sin^4 \theta_W}{(1 - 2 \sin^2 \theta_W)^2 + 4 \sin^4 \theta_W} \approx 0.2243. \quad (6)$$

Here the sine of Weinberg angle is  $\sin^2 \theta_W = 1 - M_W^2/M_Z^2$ .

The asymmetry at the c.m. energy  $\sqrt{s} = 250$  GeV has a rather flat behavior while at 500 and 1000 GeV there is some increase at  $\cos \vartheta_Z = 0.9$  value (the cut value) compared to the case at  $\cos \vartheta_Z = 0$ .

## 4 Conclusion

In this paper, we have described the evaluation of the polarization effects of the process  $e^+e^- \rightarrow \gamma Z$  at the one-loop level at high energies for future  $e^+e^-$  colliders.

The calculated polarized tree-level cross sections for the Born and hard photon bremsstrahlung were compared with the CalcHEP and WHIZARD results and very good agreement was found.

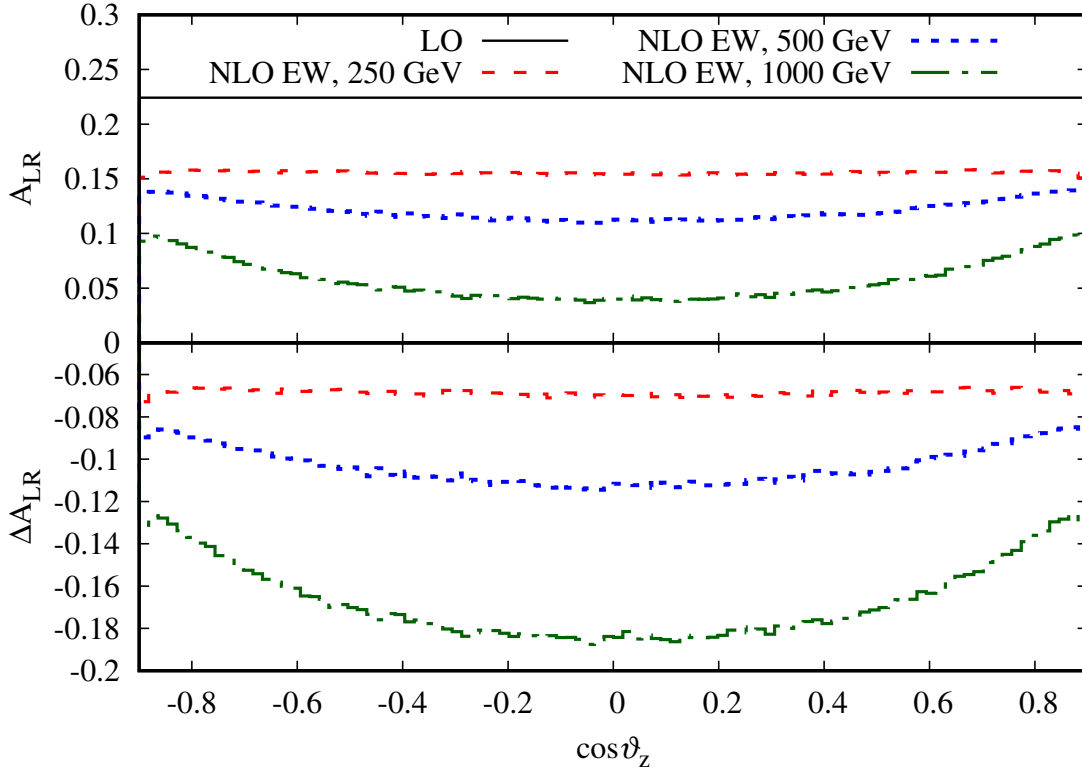


Figure 8: Distributions of left-right asymmetry  $A_{LR}$  in  $\cos\vartheta_Z$  for the Born and one-loop levels for c.m. energies  $\sqrt{s} = 250, 500, 1000$  GeV in the  $\alpha(0)$  EW scheme.

The effect of the polarization of the initial beams has been carefully analyzed for some states both for cross sections and for angular and energy distributions at the one-loop EW level, and it was found to be significant. The cross sections were found to depend strongly on the degree of polarization of the original beams. The radiative corrections themselves were rather sensitive to the degree of polarization of the initial beams and depended quite strongly on energy. In addition, calculations in the  $\alpha(0)$  and  $G_\mu$  EW schemes were considered. By combining different experimental criteria, polarization degrees of beams, and the EW schemes, radiative corrections can be minimized.

We observe a symmetric behavior of  $A_{LR}$  with respect to  $\cos\vartheta_Z = 0$ , the clear signature, the significant dependence on energy, the flatter behavior with decreasing energy and the large sensitivity to electroweak interaction effects.

## Acknowledgments

The research was supported by the Russian Foundation for Basic Research, project No. 20-02-00441 (purchasing a computing cluster) and the Russian Science Foundation, project No. 22-12-00021. We are grateful to Prof. A. Arbuzov for the help in preparation of the manuscript.

# References

- [1] A. Blondel and P. Janot, 1809.10041.
- [2] A. Blondel, A. Freitas, J. Gluza, T. Riemann, S. Heinemeyer, S. Jadach, and P. Janot, 1901.02648.
- [3] L. The LEP Collaborations ALEPH, DELPHI, OPAL, and the LEP TGC Working Group.
- [4] A. Blondel *et al.*, “Standard Model Theory for the FCC-ee: The Tera-Z”, in *Mini Workshop on Precision EW and QCD Calculations for the FCC Studies : Methods and Techniques CERN, Geneva, Switzerland, January 12-13, 2018*, 2018, 1809.01830.
- [5] FCC Collaboration, A. Abada *et al.*, *Eur. Phys. J. C* **79** (2019), no. 6 474.
- [6] ILC Collaboration, 1306.6352.
- [7] K. Fujii *et al.*, 1506.05992.
- [8] ILC Collaboration, H. Aihara *et al.*, 1901.09829.
- [9] CLICdp Collaboration, H. Abramowicz *et al.*, *JHEP* **11** (2019) 003, 1807.02441.
- [10] CEPC Study Group Collaboration, M. Dong *et al.*, 1811.10545.
- [11] Z. Duan, T. Chen, J. Gao, D. Ji, X. Li, D. Wang, J. Wang, Y. Wang, and W. Xia, *JACoW eeFACT2022* (2023) 97–102.
- [12] G. Moortgat-Pick *et al.*, *Phys. Rept.* **460** (2008) 131–243, hep-ph/0507011.
- [13] P. Bambade *et al.*, 1903.01629.
- [14] S. Bondarenko, Y. Dydyshka, L. Kalinovskaya, A. Kampf, L. Rumyantsev, R. Sadykov, and V. Yermolchyk, *Phys. Rev. D* **107** (2023), no. 7 073003, 2211.11467.
- [15] T. Mizuno, K. Fujii, and J. Tian, *AIP Conf. Proc.* **2319** (2021), no. 1 100004.
- [16] H. Aihara *et al.*, “Anomalous gauge boson interactions”, in *Electroweak symmetry breaking and new physics at the TeV scale* (T. L. Barklow, S. Dawson, H. E. Haber, and J. L. Siegrist, eds.), 3, 1995, hep-ph/9503425.
- [17] T. Mizuno, K. Fujii, and J. Tian, “Measurement of  $A_{LR}$  using radiative return at ILC 250”, in *Snowmass 2021*, 3, 2022, 2203.07944.
- [18] D. Bardin, S. Bondarenko, L. Kalinovskaya, G. Nanava, L. Rumyantsev, and W. von Schlippe, *Eur. Phys. J. C* **54** (2008) 187–197, [Erratum: *Eur.Phys.J.C* 82, 417 (2022)], 0710.3083.
- [19] A. B. Arbuzov *et al.*, *Comput. Phys. Commun. (to be published)* (2021).
- [20] R. Sadykov and V. Yermolchyk, *Computer Physics Communications* **256** (2020) 107445, 2001.10755.
- [21] M. Capdequi Peyranere, Y. Loubatieres, and M. Talon, *Nuovo Cim.* **A90** (1985) 363.

- [22] F. A. Berends, G. J. H. Burgers, and W. L. van Neerven, *Phys. Lett.* **B177** (1986) 191–194.
- [23] M. Bohm and T. Sack, *Z. Phys.* **C35** (1987) 119.
- [24] G. J. Gounaris, J. Layssac, and F. M. Renard, *Phys. Rev.* **D67** (2003) 013012, hep-ph/0211327.
- [25] A. Belyaev, N. D. Christensen, and A. Pukhov, *Comput. Phys. Commun.* **184** (2013) 1729–1769, 1207.6082.
- [26] W. Kilian, T. Ohl, and J. Reuter, *Eur. Phys. J.* **C71** (2011) 1742, 0708.4233.
- [27] W. Kilian, S. Brass, T. Ohl, J. Reuter, V. Rothe, P. Stienemeier, and M. Utsch, “New Developments in WHIZARD Version 2.6”, in *International Workshop on Future Linear Collider (LCWS2017) Strasbourg, France, October 23-27, 2017*, 2018, 1801.08034.